Membrane Biology:

Identification of Conformationally Sensitive Residues Essential for Inhibition of Vesicular Monoamine Transport by the Noncompetitive Inhibitor Tetrabenazine

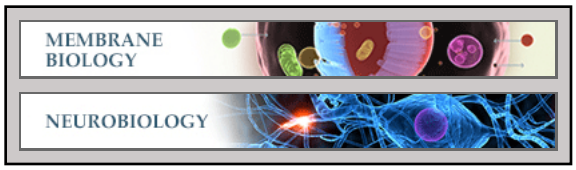

Yelena Ugolev, Tali Segal, Dana Yaffe, Yael Gros and Shimon Schuldiner

J. Biol. Chem. 2013, 288:32160-32171.
doi: 10.1074/jbc.M113.502971 originally published online September 23, 2013

THE JOURNAL OF BIOLOGICAL CHEMISTRY VOL. 288, NO. 45, pp. 32160–32171, November 8, 2013

Identification of Conformationally Sensitive Residues Essential for Inhibition of Vesicular Monoamine Transport by the Noncompetitive Inhibitor Tetrabenazine*

Received for publication, July 21, 2013, and in revised form, September 18, 2013 Published, JBC Papers in Press, September 23, 2013, DOI 10.1074/jbc.M113.502971

Yelena Ugolev[1], **Tali Segal, Dana Yaffe, Yael Gros, and Shimon Schuldiner**[2]

From the Department of Biological Chemistry, Alexander A. Silberman Institute of Life Sciences, Hebrew University of Jerusalem, 91904 Jerusalem, Israel

Background: Transport of monoamines into storage vesicles, mediated by the vesicular monoamine transporter 2 (VMAT2), is inhibited by tetrabenazine via an unknown mechanism.
Results: We identified residues essential for conformational rearrangements required for tetrabenazine binding and substrate transport.
Conclusion: Conformational rearrangements are required for binding of the inhibitor.
Significance: The results provide a novel insight into the mechanism of transport.

Vesicular monoamine transporter 2 (VMAT2) transports monoamines into storage vesicles in a process that involves exchange of the charged monoamine with two protons. VMAT2 is a member of the DHA12 family of multidrug transporters that belongs to the major facilitator superfamily of secondary transporters. Tetrabenazine (TBZ) is a non-competitive inhibitor of VMAT2 that is used in the treatment of hyperkinetic disorders associated with Huntington disease and Tourette syndrome. Previous biochemical studies suggested that the recognition site for TBZ and monoamines is different. However, the precise mechanism of TBZ interaction with VMAT2 remains unknown. Here we used a random mutagenesis approach and selected TBZ-resistant mutants. The mutations clustered around the lumenal opening of the transporter and mapped to either conserved proline or glycine, or to residues immediately adjacent to conserved proline and glycine. Directed mutagenesis provides further support for the essential role of the latter residues. Our data strongly suggest that the conserved α-helix breaking residues identified in this work play an important role in conformational rearrangements required for TBZ binding and substrate transport. Our results provide a novel insight into the mechanism of transport and TBZ binding by VMAT2.

Neuronal communication is critically dependent on the transmission of nerve impulses through chemical synapses, junctions at which electrical signals are relayed from one neuron to another via classical neurotransmitters. Accumulation of neurotransmitters in secretory vesicles, mediated by vesicular neurotransmitter transporters, allows the regulated exocytosis of neurotransmitters to the synaptic cleft (1–4). Members of the solute carrier family 18 (SLC18)[3] display vesicular activities for cationic neurotransmitters and include the vesicular monoamine transporters (VMATs) and acetylcholine transporter (VAChT) (5, 6). Two monoamine transporters, VMAT1 and VMAT2, are responsible for the uptake of dopamine, serotonin, adrenaline, noradrenaline, and histamine in a process that involves the exchange of two protons for one substrate molecule (1–3, 7). The proton electrochemical gradient ($\Delta\mu_{H+}$) necessary for transport is generated by the vacuolar-type H^+-ATPase (1).

In addition to the native substrates, VMATs interact with many clinically relevant drugs, including the psychostimulant 3,4-methylene dioxymethamphetamine and the parkinsonian toxin 1-methyl-4-phenylpyridinium (MPP^+) (7–9). Heterologous expression of VMATs protects mammalian and yeast cells against MPP^+ toxicity by sequestering the toxin in vesicles and away from its primary site of action in mitochondria (7, 10). The best characterized inhibitors of VMATs are reserpine and tetrabenazine (TBZ) (1). Reserpine is a high-affinity competitive inhibitor of VMATs and TBZ is a noncompetitive inhibitor with a significantly greater sensitivity for VMAT2. Moreover, transport substrates block TBZ binding only at concentrations 100-fold higher than their K_m values (11). These observations suggest that TBZ binds at a site distinct from substrates, and that VMAT2 exists in two different conformations: TBZ-bound or substrate-bound (11).

TBZ is a clinically relevant drug that is used for treatment of hyperkinetic disorders associated with Huntington disease and Tourette syndrome (12). Despite its therapeutic interest, the exact mode of VMAT2 interaction with TBZ remains elusive. The development of a functional expression system for rVMAT2 in *Saccharomyces cerevisiae* cells allows us to harness the power of yeast genetics to the study of the mechanism of inhibition. Screening a library of random mutants brought about the isolation and characterization of TBZ-resistant mutants that assembled near the lumenal opening of the trans-

* This work was supported, in whole or in part, by National Institutes of Health Grant NS16708.
[1] Recipient of a Lady Davis Fellowship.
[2] Mathilda Marks-Kennedy Professor of Biochemistry at the Hebrew University of Jerusalem. To whom correspondence should be addressed. Tel.: 972-2-6585992; Fax: 972-2-5634625; E-mail: Shimon.Schuldiner@huji.ac.il.
[3] The abbreviations used are: SLC18, solute carrier family 18; VMAT, vesicular monoamine transporter; MPP^+, 1-methyl-4-phenylpyridinium; TBZ, tetrabenazine; DDM, *n*-dodecyl-β-maltoside; Tricine, *N*-[2-hydroxy-1,1-bis(hydroxymethyl)ethyl]glycine; MFS, major facilitator superfamily.

porter. Strikingly, all mutants mapped to either conserved prolines or glycines, or to residues adjacent to membrane-embedded and fully conserved prolines and glycines. Our data strongly suggest that the conserved Pro and Gly residues identified in this work play an important role in conformational rearrangements required for TBZ binding and substrate transport, and provide a novel insight into the mechanism of transport and TBZ binding by VMAT2.

EXPERIMENTAL PROCEDURES

Experiments in Yeast

Yeast Strains and Plasmids—Rat *VMAT2* (rVMAT2) cDNA with hemagglutinin (HA) tag in the TM1–TM2 loop, between positions 96 and 105, and 10 His residues at the C terminus was cloned into the pAES426 yeast expression plasmid, under control of the *adh1* (alcohol dehydrogenase) promoter. The plasmid contains the *ura3* gene for selection in yeast, ampicillin-resistance marker, and a 2-μm replication in yeast (13). Cloning was done using PCR with HindIII and NotI restriction enzymes. Point mutations were produced with the QuikChange®II Site-directed mutagenesis kit (Stratagene). Plasmid pAES426 with or without His_{10} *rVMAT2* and derived mutants were routinely transformed into yeast strain ADU1–7 (US50–18C, *yor1*Δ, *snq2*D, *pdr5*Δ, *pdr10*Δ, *pdr11*Δ, *ycf1*Δ, *pdr3*Δ, *ura3*) (10). Yeast cells were transformed by the method of Elble (14).

Growth Conditions—*S. cerevisiae* cells were grown at 30 °C with shaking in standard or minimal medium. Rich medium (YPD) contained 1% Bacto-yeast extract, 2% Bacto-peptone (both from Difco), and 2% glucose. Minimal medium (S.D.) contained 0.67% Bacto-yeast nitrogen base without amino acids and 2% glucose. The SD medium was supplemented according to auxotrophic requirements (10).

Phenotype Assay on Solid Medium—For testing resistance on solid medium, *S. cerevisiae* cells were pregrown in liquid minimal medium to late log phase. Cultures were diluted to a comparable density and were decimal-diluted. Dilutions (5 μl) were spotted on YPD agar with or without the addition of the indicated concentrations of toxic compounds and inhibitors: 40 μM acriflavine, 1.5 mM MPP^+, 0.1 μM reserpine, or 2 μM TBZ. Plates were incubated for 2–3 days at 30 °C. Acriflavine, MPP^+, tetrabenazine, and reserpine were obtained from commercial sources.

Generation of Random Mutagenesis Libraries and Screening—The GeneMorph II Random Mutagenesis Kit (Agilent Technologies) was used to create a library of mutants. To generate libraries of mutants on defined regions of the gene, PCR primers with 5′- and 3′-ends annealing to the desired gene sequence were used. The product of the PCR was then used as a "megaprimer" to insert the library of mutants into the yeast expression vector.

Mutagenic libraries were transformed into competent TOP10 cells for amplification. Transformants were collected and used to prepare plasmid DNA. The amplified library (1.5 μg) was transformed into ADU1–7 cells by LiAc-heat shock transformation. The transformants were collected and 5×10^3-10^4 cells were inoculated on selective plates. Selective plates contained either 45 μM acriflavine and 2–4 μM TBZ or 1.5 mM MPP^+ and 2–4 μM TBZ, concentrations that are not permissive for cells bearing empty plasmid or wild type *rVMAT2*. Positive clones were plated on minimal medium without uracil (control for presence of the plasmid). Plasmid DNA purified from suspected clones was re-transformed into the ADU1–7 strain and transformants were re-tested for their ability to grow on selective medium. The sequences of all constructs were verified by DNA sequencing.

Experiments in HEK293 Cells

Plasmids, Cell Culture, and Transfection—*rVMAT2* cDNA with hemagglutinin (HA) tag in the second loop, between positions 96 and 105, and 10 His residues at the C terminus was cloned into pcDNA3.1 plasmid (Invitrogen) using PCR, with HindIII and NotI restriction enzymes (15). Subcloning of isolated mutants from the pAES426 vector was done with SanDI and NotI restriction enzymes. Growth of HEK293 cells and rVMAT2 expression was done as previously described (15).

Reconstitution into Proteoliposomes—Reconstitution was done essentially as previously described (15). Specifically, HEK293 cells transfected with the appropriate mutant were quickly thawed in 37 °C and kept on ice. *n*-Dodecyl-β-maltoside (DDM; Glycon) and polar brain lipids (Avanti Polar Lipids, Inc., Alabaster, AL) were added to a final concentration of 2% and 0.5 mg/ml, respectively. After 15 min of shaking at 4 °C, cells were sonicated 90 s in a ice-cold bath-type sonicator and then incubated for 1 h at 4 °C with rotation. The suspension was centrifuged for 15 min at 20,000 × *g* at 4 °C and the supernatant was incubated with nickel-nitrilotriacetic acid beads (Qiagen, Hilden, Germany) equilibrated with 150 mM NaCl, 15 mM Tris-HCl, pH 7.5 (Na buffer), and 0.08% DDM in the presence of 10 mM imidazole for 1 h at 4 °C. Beads were then loaded onto a column, washed once with 10 volumes of Na buffer with 0.08% DDM, 0.5 mg/ml of polar brain lipid, and 10 mM imidazole, and washed three times with 10 volumes of the same solution that contained 1% octyl glucoside instead of DDM. rVMAT2 was eluted using Na buffer with 1% octyl glucoside, 0.5 mg/ml of polar brain lipid, and 450 mM imidazole. The solubilized protein was mixed with an equal volume of reconstitution mixture containing Na buffer, 1.2% octyl glucoside, 10 mg/ml of polar brain lipids, and 1 mg/ml of asolectin, and sonicated to clarity in a bath-type sonicator. The mixture was then dialyzed at 4 °C against 300 volumes of ammonium buffer containing 140 mM $(NH_4)_2SO_4$ + 15 mM Tris-SO_4, pH 7.4. After overnight dialysis the external buffer was replaced with fresh buffer for an additional 2 h of dialysis. The liposomes mixture was then ultracentrifuged at 213,500 × *g*, 70 min, 4 °C. The supernatant was discarded and the liposome pellet was re-suspended in 150 μl of ammonium buffer, divided into aliquots, frozen in liquid air and kept at −70 °C until use.

Uptake of [^{3}H]Serotonin in Proteoliposomes—Liposomes were thawed and sonicated to clarity in a bath-type sonicator. The uptake assay was performed in reaction buffer containing 140 mM K_2-tartrate, 10 mM Tricine, 10 mM Tris, and 5 mM $MgCl_2$, pH 8.5. Liposomes (1 μl) were diluted into 200 μl of reaction buffer with 50 nM valinomycin and the indicated concentrations of the radiolabeled serotonin, usually 100 nM [^{3}H]serotonin (PerkinElmer Life Sciences). Nonspecific accu-

mulation of [^{3}H]serotonin was measured in the presence of 5 μM reserpine or 15 μM nigericin and subtracted from the total transport. The reaction was stopped at the indicated time points by dilution of the mixture in 2 ml of ice-cold buffer and filtered on 0.22-μm GSWP (Millipore) filters. Radioactivity was measured using liquid scintillation.

Binding of [^{3}H]TBZOH in Proteoliposomes—Liposomes (1–2 μl) were added to 200 μl of reaction buffer containing 150 mM NaCl, 15 mM Tris-HCl, pH 7.5, and increasing concentrations of [^{3}H]TBZOH (American Radiolabeled Chemicals, St. Louis, MO; 6 Ci/mmol, and Vitrax Radiochemicals, 20 Ci/mmol) at room temperature. The reaction was stopped after 20 min by dilution in ice-cold buffer with 125 μM tetrabenazine and was filtered through 0.22-μm GSWP filters (Millipore) presoaked with 125 μM tetrabenazine. Nonspecific binding measured in the presence of 125 μM tetrabenazine was subtracted from the total binding levels.

Protein Determination in Proteoliposomes—Proteoliposomes were solubilized in 2% DDM and 10 μl were spotted on PVDF membranes (Millipore, Billerica, MA). The membrane was then blocked for 1 h in 2% BSA in TBST (137 mM NaCl, 50 mM Tris, and 0.05% Tween 20). The blot was then incubated overnight with 1:5000 dilution of a mouse monoclonal antibody against the HA epitope (12CA5; BAbCo, Berkeley, CA). After five washes with TBST, the blot was incubated with DyLight-conjugated donkey anti-mouse IgG (Jackson ImmunoResearch Laboratories, West Grove, PA) diluted 1:4000 and imaged using MF-chemibis 32 (DNR, Israel). Protein amounts were quantified using Gel-Quant software.

RESULTS

Glycine 308 Is Essential for TBZ Binding—We recently established an expression system of rVMAT2 in the *S. cerevisiae* ADU1–7 mutant strain, in which seven major genes coding for the ATP-binding cassette (ABC) transporters were inactivated, rendering it sensitive to several toxic compounds (16). Expression of rVMAT2 in ADU1–7 cells conferred resistance against two substrates, namely MPP^+ and acriflavine (10), and allowed us to apply a method of directed evolution for isolation of mutants with altered affinity to TBZ. All mutations in our previous study mapped to TM2 (F136L) and TM11 (I425F, V428A). To try to identify other parts of the transporter involved in TBZ binding, we applied selective pressure on specifically defined segments of the gene. To do so, a segment encompassing a region encoding for TM3 through TM10 was subjected to the random mutagenesis. A library containing these random mutants was prepared and transformed into the ADU1–7 strain. The genetic screen based on positive selection was performed using selective plates containing acriflavine supplemented with TBZ, conditions under which wild type rVMAT2 does not support growth (Ref. 10 and Fig. 1*A*, WT). The screen revealed an interesting mutant at position Gly^{308} (TM7). The results of a phenotypic analysis shown in Fig. 1*A* reveal that yeast cells expressing rVMAT2-G308A preserved their capacity to grow in the presence of MPP^+ and acriflavine. However, replacement of Gly^{308} by a relatively conserved alanine conferred a remarkable resistance to the inhibitor TBZ in the presence of both toxic compounds (Fig. 1*A*, *+TBZ*).

Because the expression levels of rVMAT2 in yeast cells are very low (10), we chose the HEK293 expression system for further biochemical analysis (15, 17). The rVMAT2-G308A mutant was subcloned into pcDNA3 vector, expressed in HEK293 cells and reconstituted in proteoliposomes loaded with ammonium sulfate. A pH gradient (acidic inside) is generated by dilution of the proteoliposomes to an ammonium-free medium containing radiolabeled serotonin (5-hydroxytryptamine). Protein content of each batch of proteoliposomes was estimated by dot blot as shown in Fig. 2. The transport activity of the rVMAT2-G308A mutant for [^{3}H]serotonin was first measured in a time course assay and was found to be similar to that exhibited by the wild type (Fig. 1*B*). A more detailed kinetic analysis demonstrated that the K_m value for serotonin transport by the G308A replacement was similar to that of the wild type protein, whereas the V_{max} was higher (Fig. 1*D*). To determine whether the G308A substitution affects sensitivity to the competitive inhibitor reserpine, we measured the IC_{50} values for serotonin uptake inhibition by reserpine. We found that the mutant retained its sensitivity to reserpine (Fig. 1*D*). In contrast, the IC_{50} value of the G308A mutant for TBZ was dramatically modified from that of the wild type (Fig. 1*D*). The mutant showed a dramatic decrease in affinity to [^{3}H]TBZOH, an analog of TBZ. Thus, whereas the K_D value for [^{3}H]TBZOH binding for the wild type was 5.2 ± 0.8 nM, for the G308A mutant it was >100 nM (Fig. 1*D*). The K_D of the mutant could not be determined accurately because of the low levels of binding and the fact that it did not saturate in the concentration range measured. This drastic reduction in TBZ affinity is in good agreement with the TBZ-resistant phenotype observed in yeast. Altogether, the results support the contention that Gly^{308} is critical for TBZ binding, but is not essential for serotonin transport and reserpine binding.

The Role of Glycine 308 in TBZ Binding—To further understand the role of Gly^{308} in TBZ binding, we compared the sequences of SLC18 family members (Fig. 1*C*). Multiple sequence alignment shows that while in VMATs Gly^{308} is conserved, in VAChT transporters, a proline residue is in a position that corresponds to Gly^{308} in VMATs. Because glycine residues are unique in their ability to adopt a wide range of main chain dihedral angles and prolines tend to destabilize α-helices by a lack of a backbone hydrogen bond (18), we hypothesized that G308A replacement abolished the α-helix flexibility required for TBZ binding. To examine this notion, we attempted to recover the sensitivity to TBZ by introducing the α-helix-breaking proline at this position. The G308P mutant was first tested in the phenotype assay in yeast. As seen in Fig. 1*A*, cells expressing rVMAT2-G308P displayed a significant ability to grow in the presence of MPP^+ and acriflavine, but were unable to support growth in the presence of TBZ, suggesting that the G308P mutation restored TBZ sensitivity of the transporter. Biochemical analysis of the G308P mutant reconstituted in proteoliposomes revealed that the ability of the rVMAT2-G308P mutant to transport serotonin in a time course assay was higher than that observed for the wild type (Fig. 1*B*). The K_m and V_{max} values determined for the G308P mutant were higher than those of the wild type, ~2- and ~4-fold, respectively. Most importantly, further biochemical analysis yielded K_D for

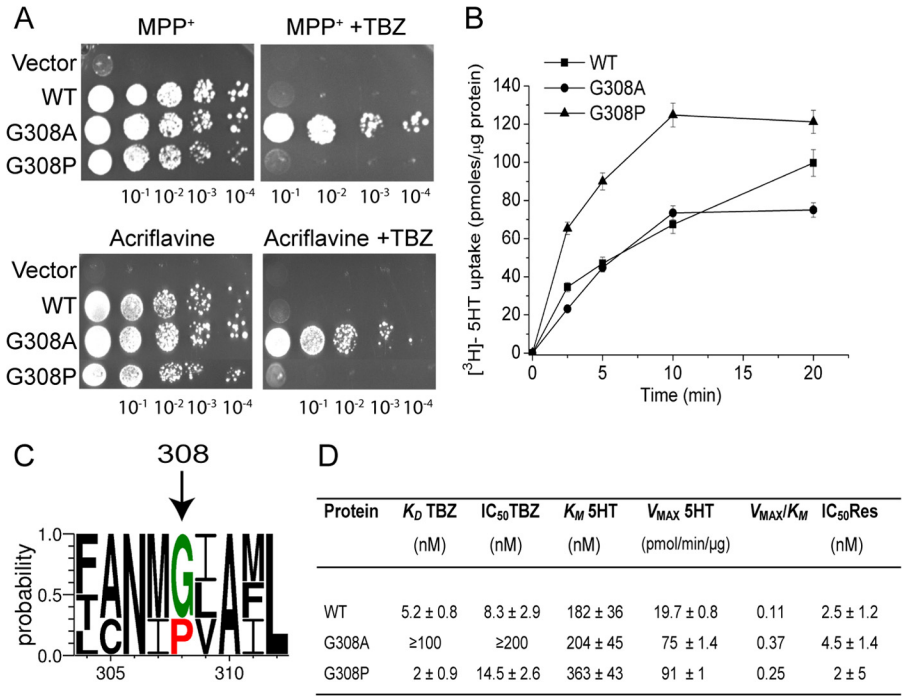

Protein	K_D TBZ (nM)	IC_{50}TBZ (nM)	K_M 5HT (nM)	V_{MAX} 5HT (pmol/min/µg)	V_{MAX}/K_M	IC_{50}Res (nM)
WT	5.2 ± 0.8	8.3 ± 2.9	182 ± 36	19.7 ± 0.8	0.11	2.5 ± 1.2
G308A	≥100	≥200	204 ± 45	75 ± 1.4	0.37	4.5 ± 1.4
G308P	2 ± 0.9	14.5 ± 2.6	363 ± 43	91 ± 1	0.25	2 ± 5

FIGURE 1. **Gly^{308} functions as a pivotal molecular hinge required for TBZ binding.** *A,* replacement of Gly^{308} by Ala (G308A) confers resistance to TBZ in yeast cells, whereas a Pro replacement rescues TBZ-resistant phenotype. ADU1–7 cells transformed with pAES426 (empty vector) or pAES426 harboring either rVMAT2 or Gly^{308} mutants were grown in minimal medium and diluted to comparable densities. 5 µl of serial dilutions of the culture were spotted on rich solid medium (YPD) supplemented with 1.5 mM MPP^+ (*upper panel*), or 40 µM acriflavine (*lower panel*). Where indicated, the plates contained 2 µM TBZ. Growth was analyzed after 48 h at 30 °C. The plates are representative of at least three independent experiments. *B,* time course of [^{3}H]serotonin ([^{3}H]*5HT*) transport by Gly^{308} mutants reconstituted in proteoliposomes. The uptake assay was performed as described under "Experimental Procedures." Ammonium-loaded proteoliposomes (1 µl) were diluted into 200 µl of reaction buffer to generate the pH gradient that drives serotonin transport and 50 nM valinomycin was added to prevent the generation of a membrane potential by the electrogenic exchange of $2H^+$ with one serotonin molecule. All data are mean ± S.E. of 2–3 experiments. *C,* multiple sequence alignment of members of the SLC18 family in the region of residues 304–312 (*TM7*). Multiple alignment was performed using Clustal Omega (38). A conservation logo was created using WebLogo 3.3 (39, 40). Only a fraction of the alignment corresponding to residues 304–312 is shown. *D,* kinetic properties of rVMAT2 and Gly^{308} mutants. Proteoliposomes were prepared from HEK293 cells expressing either rVMAT2 or Gly^{308} mutants. Protein determination and serotonin uptake in proteoliposomes and [^{3}H]TBZOH binding were performed as described under "Experimental Procedures." The "specificity constant" V_{max}/K_m was obtained by simply dividing the corresponding values given in the table and the units are those shown. TBZ sensitivity was assessed by calculating the amount of ligand required to inhibit serotonin transport by 50% (IC_{50}). The uptake assay was performed in the presence of increasing concentrations of TBZ (0–200 nM) for 20 min. Reserpine sensitivity was assessed by calculating the concentration required to inhibit serotonin transport by 50% (IC_{50}) (0–100 nM).

[^{3}H]TBZOH and IC_{50} values for TBZ similar to that measured for the wild type (Fig. 1*D*). The results described support the contention that the flexibility conferred by Gly^{308} is important for TBZ binding. Thus, we conclude that one important role of Gly^{308} is to provide a functional conformational flexibility required for TBZ binding.

The Role of Proline 314 in TBZ Binding and Substrate Transport—All our previous screening studies were performed with acriflavine as the toxic substrate. Acriflavine differs in size and structure from the native substrates of VMAT2 (Fig. 3), and therefore its binding determinants may differ from those of the monoamines. Early binding data suggested that TBZ and transportable substrates interact with VMAT2 at distinct sites (1, 11). However, mutagenesis studies showed that replacements at several positions reduced the affinity of rVMAT2 for TBZ and affected the kinetic properties of the transport of serotonin (10, 15, 19, 20). The apparent discrepancy with previous reports suggested interaction at distinct sites may be due to the fact that substrates and TBZ bind to different conformations, despite shared binding site determinants. MPP^+ is a well characterized substrate of VMATs, shown experimentally to interact with the transporter at a site similar or in the vicinity of that occupied by its native ligands (21). Therefore, in an attempt to gain further understanding on the relationships between TBZ and substrate binding sites, we also used MPP^+ as the toxic substrate in our genetic screens for TBZ-resistant variants. The library described above, comprising rVMAT2 harboring mutations at the gene segment encoding for TM3–10, was transformed into the ADU1–7 strain. The genetic screen based on positive selection was performed using selective plates containing MPP^+ supplemented with TBZ. The screen revealed TBZ-resistant mutants bearing two different replacements at the same position, namely P314L and P314T (TM7). Although both mutants displayed substantial growth in the presence of MPP^+ (Fig. 4*A*), their ability to confer resistance against acriflavine was significantly lower than that of the wild type and resistance to TBZ was undetectable under these conditions (Fig. 4*A*). These results explain why Pro^{314} was not isolated when acriflavine was used in the screen.

For further biochemical analysis rVMAT2-P314L and P314T mutants were expressed in HEK293 cells and proteoliposomes were prepared. In a time course assay, the rate of serotonin transport by the rVMAT2-P314L mutant is higher than that observed with the wild type protein (Fig. 4*B*). In contrast, the transport activity for the P314T substituent was significantly reduced. Strikingly, further analysis revealed that both replace-

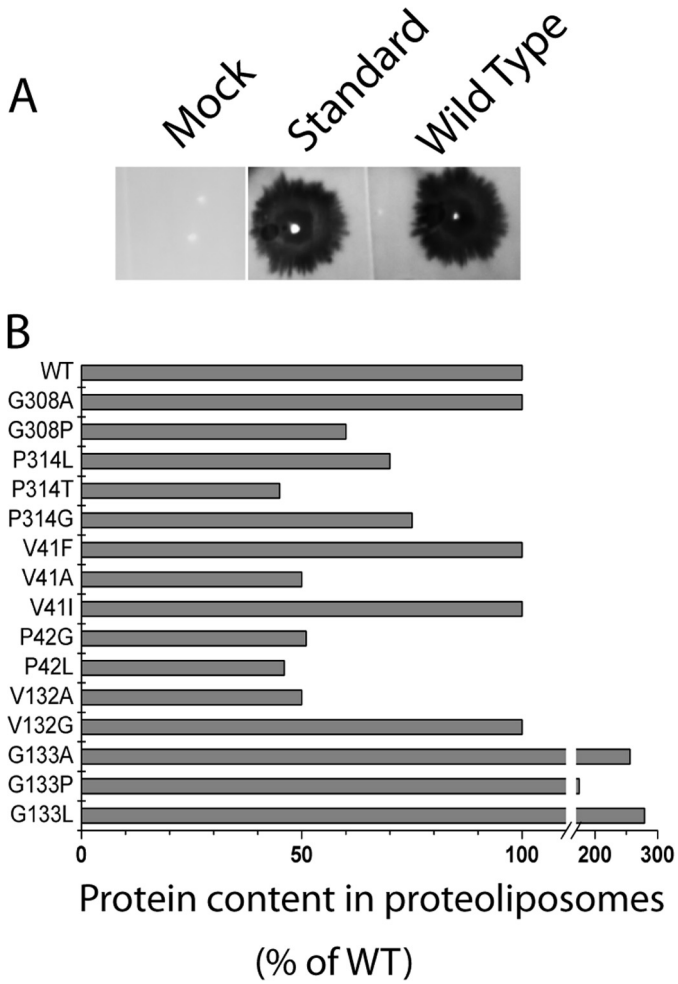

FIGURE 2. **Determination of protein amounts in proteoliposomes.** *A,* typical result of the dot blot experiment. rVMAT2-WT overexpressed in SF9 cell and purified to homogeneity served as a standard and positive control. The dot blot was performed as described under "Experimental Procedures." *B,* quantification of protein amounts in rVMAT2 mutants. The amount of protein is expressed as the percent of wild type. The results shown are representative and for specific batches used for determination of K_m and V_{max} throughout the paper.

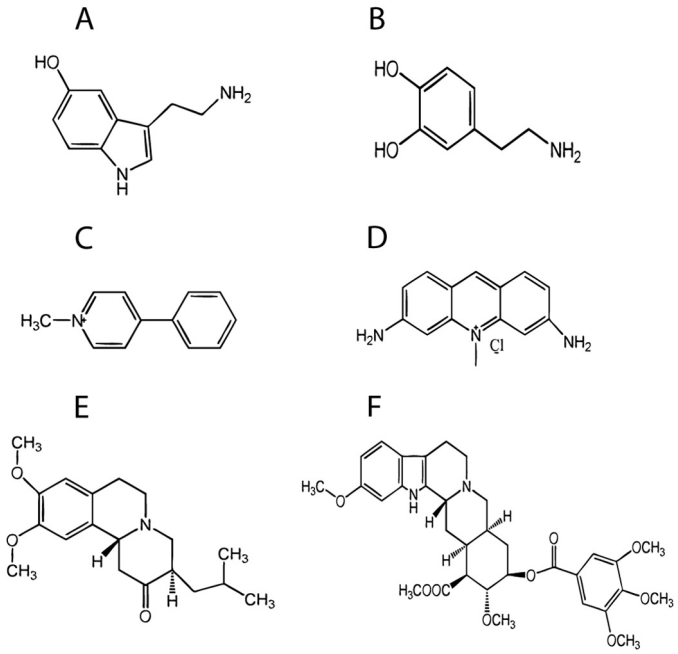

FIGURE 3. **Chemical structure of selected substrates and inhibitors of wild type VMAT2.** *A,* serotonin; *B,* dopamine; *C,* MPP^+; *D,* acriflavine; *E,* tetrabenazine; *F,* reserpine.

ments had a dramatic effect on the kinetic properties of serotonin transport (Fig. 4*D*). Noteworthy, the K_m and V_{max} values were increased up to ~5- and ~10-fold, respectively, for the P314L mutant, compared with the wild type. Transport by the P314T was too low to allow the accurate determination of K_m and V_{max} values and the K_m is most likely higher than 2000 nM. As expected from the phenotype, the affinity to TBZ was dramatically reduced in both mutants. Thus, K_D values determined for [^{3}H]TBZOH binding calculated for both mutants were >100 nM, and IC_{50} values for TBZ were >200 nM (Fig. 4*D*). Yet, we found that the mutations at position Pro^{314} did not significantly alter the apparent affinity to reserpine, as estimated from its ability to inhibit serotonin transport (Fig. 4*D*). Based on these results, we propose that a Pro residue at position 314 is necessary for TBZ binding and maintaining kinetic properties of the wild type transporter.

Pro^{314} Is Irreplaceable for TBZ Binding—Multiple sequence alignment shows that Pro^{314} is fully conserved in the SLC18 family (Fig. 5*A*) and is highly conserved among its bacterial homologues from the major facilitator superfamily (MFS) family (Fig. 4*C*). The sequence data suggests that the presence of proline at this position may be critical for function. We hypothesized that Pro^{314} may create a kink contributing to conformational movements of the transporter and that a glycine residue should be able to functionally substitute for the proline at this position. Therefore, we introduced the point mutation P314G into rVMAT2 and expressed it in yeast. As seen in Fig. 4*A*, the rVMAT2-P314G mutant maintained a substantial resistance to MPP^+, but was unable to recover TBZ sensitivity of the transporter.

rVMAT2-P314G mutant reconstituted in proteoliposomes displayed substantial transport activity in a time course assay (Fig. 4*B*). Also in the case of the P314G substitution, further biochemical analysis revealed a dramatic increase in K_m and V_{max} values (Fig. 4*D*). These observations further confirm the functional importance of Pro^{314} in the transport mechanism of rVMAT2. Moreover, as was anticipated from the TBZ-resistant phenotype in yeast, the ability of P314G to bind TBZ was impaired and the K_D and IC_{50} values for TBZ were too high to be determined as observed for P314L and P314T variants (Fig. 4*D*).

Valine 41 Is Essential for TBZ Binding and Substrate Transport—Previous photoaffinity labeling studies suggested that the cytosolic N terminus and TM1 might comprise residues involved in the binding of TBZ (22, 23). To identify binding sites at the N-terminal bundle a region encompassing the cytosolic N terminus and TMs 1–6 was subjected to random mutagenesis. A library containing the random mutants was prepared and transformed into the ADU1–7 strain. The genetic screen was performed as above using selective plates containing MPP^+ supplemented with TBZ. The screen gave rise to three new TBZ-resistant mutants. In two cases, the plasmids carried two

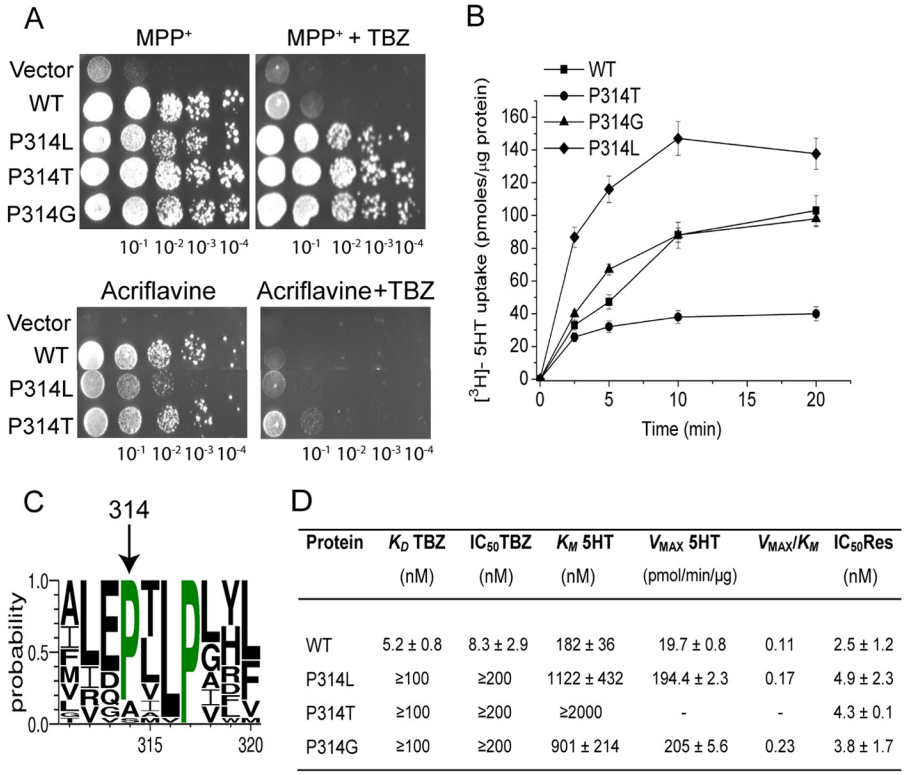

Protein	K_D TBZ (nM)	IC_{50}TBZ (nM)	K_M 5HT (nM)	V_{MAX} 5HT (pmol/min/µg)	V_{MAX}/K_M	IC_{50}Res (nM)
WT	5.2 ± 0.8	8.3 ± 2.9	182 ± 36	19.7 ± 0.8	0.11	2.5 ± 1.2
P314L	≥100	≥200	1122 ± 432	194.4 ± 2.3	0.17	4.9 ± 2.3
P314T	≥100	≥200	≥2000	-	-	4.3 ± 0.1
P314G	≥100	≥200	901 ± 214	205 ± 5.6	0.23	3.8 ± 1.7

FIGURE 4. **The highly conserved Pro^{314} is crucial for TBZ binding and plays a role in the transport function of rVMAT2.** *A,* replacement of Pro^{314} by Leu or Thr confers resistance to TBZ in yeast cells. ADU1–7 cells were transformed with pAES426 (empty vector) or pAES426 harboring rVMAT2 and Pro^{314} mutants. Growth was assayed and analyzed as described in the legend to Fig. 1*A*. *B,* time course of [^{3}H]serotonin transport by Pro^{314} mutants reconstituted in proteoliposomes. The uptake assay was performed as described in the legend to Fig. 1*B*. All data are mean ± S.E. of 2–3 experiments. *C,* conservation of Pro^{314}. The sequence of rVMAT2 was used to query the National Center for Biotechnology Information (NCBI) using the psi-BLAST tool as provided by the NCBI server with default parameters. Multiple sequence alignment and the conservation logo were created as described in the legend to Fig. 1*C*. Only a fraction of the alignment corresponding to residues 311–320 is shown. *D,* kinetic properties of Pro^{314} mutants. Proteoliposomes were prepared from HEK293 cells expressing rVMAT2 or Pro^{314} mutants. K_D for [^{3}H]TBZOH binding, K_m, V_{max} for [^{3}H]serotonin uptake, and IC_{50} for reserpine and TBZ, were determined as described in the legend to Fig. 1*D*.

mutations (V41F/R10P and V132A/L270F, respectively). They were separated, the phenotypes of each mutant were tested and it was found that the single mutations at positions Val^{41} (V41F) and Val^{132} (V132A) were the ones responsible for TBZ insensitivity. The third plasmid carried a single mutation that resulted in replacement of Val^{132} with Gly.

Substitution of the smaller isopropyl group of Val^{41} with the phenyl group of phenylalanine significantly impaired pharmacological properties of wild type rVMAT2. Thus, the ability of the rVMAT2-V41F mutant to support growth in the presence of MPP^+ was reduced (Fig. 6*A*) and resistance against acriflavine was practically eliminated (Fig. 6*A*, *lower panel*). Subsequent biochemical analysis in proteoliposomes demonstrated that serotonin transport activity in the V41F mutant was practically undetectable (Fig. 6*B*). It is likely that the residual growth observed in the presence of MPP^+ is due to a slow and technically undetectable level of transport into the large yeast vacuole. The ability of the mutant to bind TBZ was also dramatically impaired. Thus, the K_D value measured for the rVMAT2-V41F mutant was >100 nM, compared with 5.2 ± 0.8 nM calculated for the wild type.

Multiple sequence alignment shows that Val^{41} is fully conserved in the SLC18 family (Fig. 5*B*) and is only moderately conserved among its related bacterial homologues (Fig. 6*C*). Remarkably, Val^{41} is immediately adjacent to the highly conserved P*XX*P sequence (Fig. 6*C*), which is part of the motif D2. Motif D2 is located in TM1 and conserved in the MFS family (24, 25). To further investigate the role of Val^{41} in TBZ binding

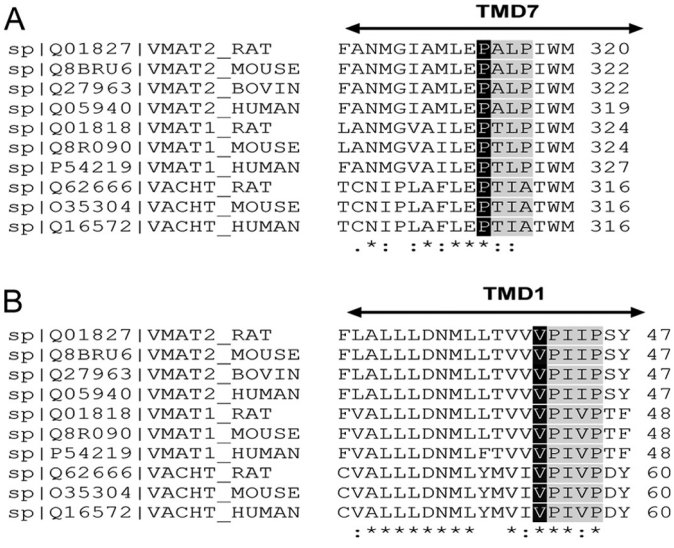

FIGURE 5. **Multiple sequence alignment of the members of SLC18 family.** *A,* alignment in the region of residues 304–320 (*TM7*). *B,* alignment in the region of residues 27–47 (*TM1*). Multiple sequence alignment was performed as described in the legend to Fig. 1*C*. Pro^{314} and Val^{41} are highlighted in *black*. P*XX*P domains are highlighted in *gray*.

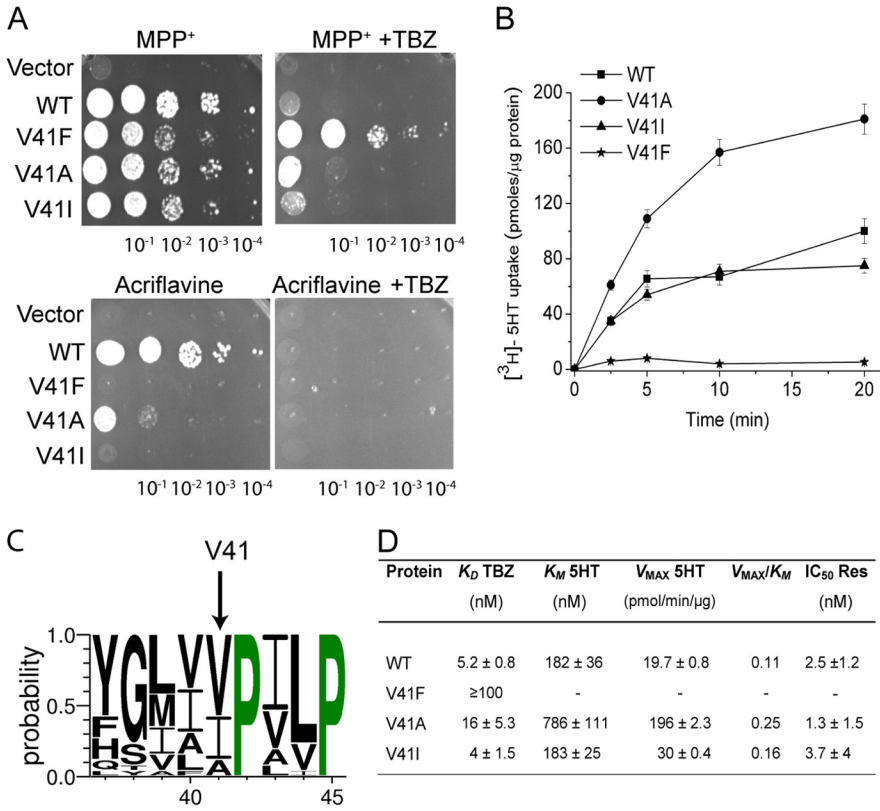

Protein	K_D TBZ (nM)	K_M 5HT (nM)	V_{MAX} 5HT (pmol/min/µg)	V_{MAX}/K_M	IC_{50} Res (nM)
WT	5.2 ± 0.8	182 ± 36	19.7 ± 0.8	0.11	2.5 ±1.2
V41F	≥100	-	-	-	-
V41A	16 ± 5.3	786 ± 111	196 ± 2.3	0.25	1.3 ± 1.5
V41I	4 ± 1.5	183 ± 25	30 ± 0.4	0.16	3.7 ± 4

FIGURE 6. **Substitution of the conserved amino acid Val[41] by Phe impairs the pharmacological properties of rVMAT2.** *A,* the V41F mutation confers resistance to TBZ and eliminates the ability to support growth on acriflavine. ADU1–7 cells were transformed with pAES426 (empty vector) or pAES426 harboring rVMAT2 or Val[41] mutants. Where indicated, the plates contained 2 μM TBZ. Growth was assayed and analyzed as described in the legend to Fig. 1*A*. *B,* time course of [^{3}H]serotonin transport by Val[41] mutants reconstituted in proteoliposomes. The uptake assay was performed as described in the legend to Fig. 1*B*. *C,* conservation of Val[41]. A conservation logo was created as described in the legend to Fig. 4*C*. Only a fraction of the alignment corresponding to residues 37–45 is shown. *D,* kinetic properties of Val[41] mutants. Proteoliposomes were prepared from HEK293 cells expressing rVMAT2 and Val[41] mutants. K_D for [^{3}H]TBZOH binding, K_m, V_{max} for [^{3}H]serotonin uptake, and IC_{50} for reserpine, were determined as described in the legend to Fig. 1*D*.

and substrate recognition, we undertook a mutational analysis of this position. Because many bacterial homologues contain at this position residues with relatively small non-polar side chains, namely Val, Ala, and Ile (Fig. 6*C*), we constructed rVMAT2-V41A and -V41I mutants and tested them in ADU1–7 yeast strains for their ability to confer resistance to rVMAT2 substrates. As seen in Fig. 6*A*, V41A and V41I mutants conferred a significant, albeit reduced, resistance to MPP^+ (Fig. 6*A*). The capacity to support growth on acriflavine was detectable, and barely so, only in the V41A mutant (Fig. 6*A*, *lower panel*). Interestingly, V41A and V41I mutants displayed a TBZ-sensitive phenotype on the MPP^+ background, suggesting that these replacements maintain the ability of the transporter to bind TBZ.

Transport of serotonin was assayed in proteoliposomes where V41A and V41I displayed activities comparable with that observed for the wild type (Fig. 6*B*). The K_m and V_{max} values determined for the V41I mutant were comparable with that of the wild type (Fig. 6*D*). In contrast, V41A replacement exerted a more profound effect on the kinetic parameters of the transporter, causing a significant increase in K_m and V_{max} values (~4 to ~10-fold higher than wild type). The V41I mutant displayed an affinity to [^{3}H]TBZOH comparable with that of the wild type, whereas that of the V41A mutant was ~3-fold lower, still in the same order of magnitude (Fig. 6*D*). The sensitivity to reserpine was preserved in all mutants tested (Fig. 6*D*). Our results indicate that bulky (Phe) side chains at this position strongly affect serotonin transport activity and TBZ binding.

V132A and V132G Mutations Produce Deleterious Effects on rVMAT2 Function—The other two TBZ-resistant mutants isolated in the same screen described above were V132A and V132G. Fig. 7*A* demonstrates that rVMAT2-V132A and V132G mutants conferred a substantial resistance against MPP^+, whereas the capacity to grow in the presence of acriflavine was somewhat reduced (Fig. 7*A*). Both replacements exhibited TBZ-resistant phenotypes in the presence of MPP^+, whereas almost no growth on the plates containing acriflavine and TBZ was observed (Fig. 7*A*). Noteworthy, we found that both replacements allowed for some (V132A) or full (V132G) growth in the presence of MPP^+ and reserpine (Fig. 7*A*).

Both replacements significantly altered serotonin transport assayed in proteoliposomes (Fig. 7*B*) and the K_m values for V132G and V132A mutants were increased (Fig. 7*D*). The V_{max} determined for V132G was similar to that of the wild type transporter. However, due to the dramatic increase in K_m, the replacement catalyzes a very inefficient process. The V_{max} of the V132A mutant was too low to be determined accurately enough (Fig. 7*D*). Although the rVMAT2-V132A mutant exhibited a significant reduction in the affinity for TBZ and reserpine, the ability to bind either of the inhibitors tested was

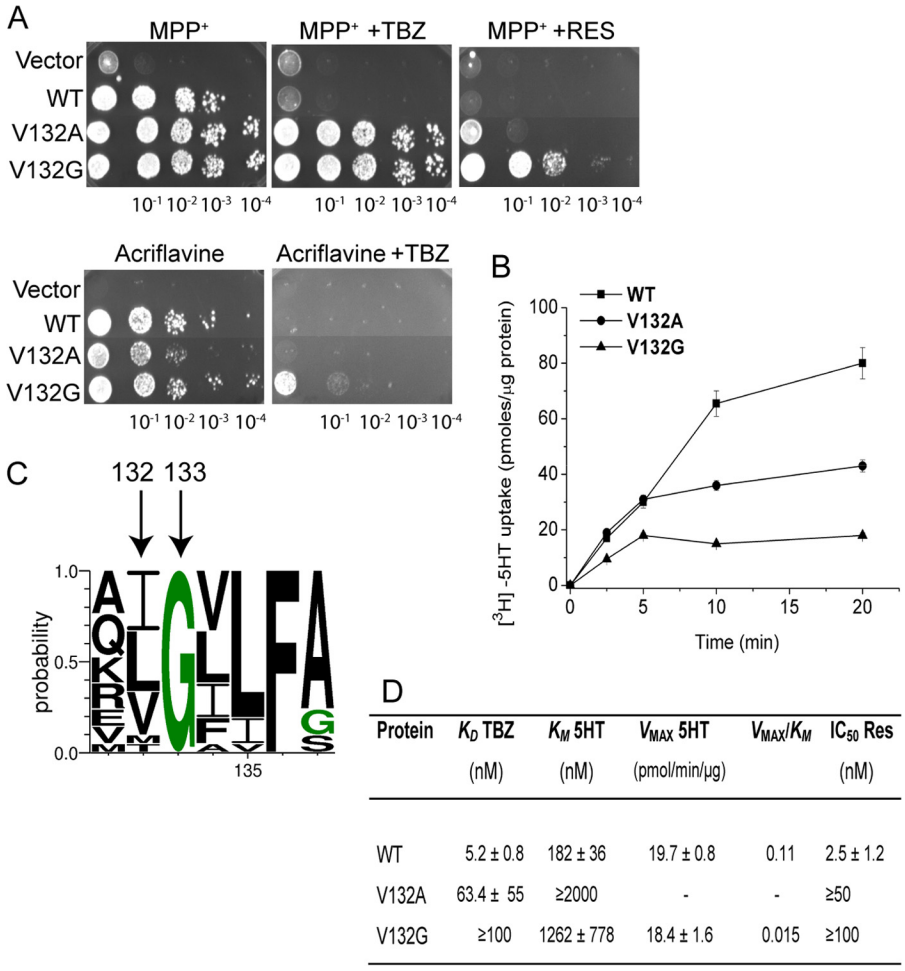

Protein	K_D TBZ (nM)	K_M 5HT (nM)	V_{MAX} 5HT (pmol/min/µg)	V_{MAX}/K_M	IC_{50} Res (nM)
WT	5.2 ± 0.8	182 ± 36	19.7 ± 0.8	0.11	2.5 ± 1.2
V132A	63.4 ± 55	≥2000	-	-	≥50
V132G	≥100	1262 ± 778	18.4 ± 1.6	0.015	≥100

FIGURE 7. **Val^{132} is important for the binding and transport activity of rVMAT2.** *A,* mutations of Val^{132} cause TBZ and reserpine-resistant phenotypes in yeast. ADU1–7 cells were transformed with pAES426 (empty vector) or pAES426 harboring rVMAT2 or Val^{132} mutants. Where indicated, the plates contained 2 μM TBZ or 0.1 μM reserpine. Growth was assayed and analyzed as described in the legend to Fig. 1*A*. *B,* time course of [^{3}H]serotonin transport by Val^{132} mutants reconstituted in proteoliposomes. The uptake assay was performed as described in the legend to Fig. 1*B*, except that nonspecific accumulation of [^{3}H]serotonin was measured in the presence of 15 μM nigericin, which disrupts the proton gradient, and was subtracted from the total transport. *C,* conservation of Val^{132}. A conservation logo was created as described in the legend to Fig. 4*C*. Only a fraction of the alignment corresponding to residues 131–137 is shown. *D,* kinetic properties of Val^{132} mutants. Proteoliposomes were prepared from HEK293 cells expressing rVMAT2 and Val^{132} mutants. K_D for [^{3}H]TBZOH binding, K_m, V_{max} for [^{3}H]serotonin uptake, and IC_{50} for reserpine were determined as described in the legend to Fig. 1*D*.

completely eliminated by the V132G substitution (Fig. 7*D*). Importantly, multiple sequence alignment revealed that Val^{132} is immediately adjacent to Gly^{133}, which is fully conserved in the SLC18 family and among its bacterial homologues from the MFS family (Fig. 7*C*). Our results indicate that Val^{132} is critical for reserpine and TBZ binding and serotonin transport activity of the transporter.

Site-directed Mutagenesis of Conserved Pro and Gly Residues Adjacent to Val^{41} and Val^{132} Reveal Their Important Roles—The observations described above point to the significant role of two residues, Val^{41} and Val^{132}, immediately adjacent to highly conserved α-helix breakers glycine and proline. The Pro residue equivalent to Pro^{42} was previously shown in rVMAT1 to be important for activity (26). Therefore, we generated additional mutants by site-directed mutagenesis, namely P42G and P42L, and studied their properties in proteoliposomes. As previously shown for VMAT1 (26), the P42G mutant displays levels of serotonin transport activity similar to the wild type, whereas the transport activity of the P42L substitution is undetectable (Fig. 8*A*). Both substitutions lost the high affinity binding of TBZ almost entirely (Fig. 8*C*).

Replacement of the fully conserved Gly^{133} with Ala, Leu, or Pro resulted in the almost complete loss of serotonin transport (Fig. 8*B*). High affinity binding of TBZ was undetectable in the Leu and Pro mutations and significantly decreased in the case of the Ala replacement with a K_D of 15.3 ± 2.1 nM (Fig. 8*C*).

Clustering of the Mutations in the Model of rVMAT2—Based on structural conservation we generated a homology model of rVMAT2 with a crystal structure of LacY in the C_{in} conformation serving as a template (15). This model has the standard MFS-fold, that is, with two domains of 6 transmembrane (TM) helices each, related by 2-fold pseudo symmetry whose axis runs normal to the membrane and between the two halves (27–29) (Fig. 9*B*). According to the alternating access mechanism, a single binding site is alternately exposed, by conformational change, to either side of the membrane (30, 31). In several families of secondary transporters, including the MFS, the basis for the alternating access mechanism arises from swapping of con-

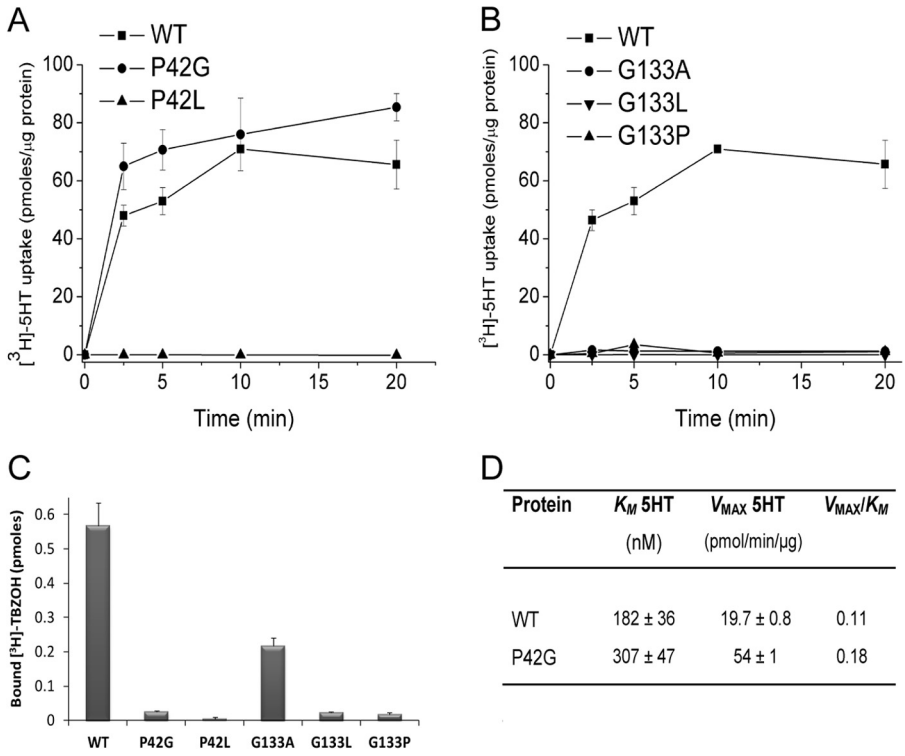

FIGURE 8. **[^{3}H]Serotonin transport and [^{3}H]TBZOH binding by Pro^{42} and Gly^{133} mutants reconstituted in proteoliposomes.** The uptake assay was performed as described in the legend to Fig. 1*B*, except that nonspecific accumulation of [^{3}H]serotonin was measured in the presence of 15 μM nigericin, which disrupts the proton gradient, and was subtracted from the total transport. *A* and *B*, time course for the Pro^{42} and Gly^{133} replacements, respectively; *C*, binding of [^{3}H]TBZOH; *D*, kinetic constants of P42G and G133A.

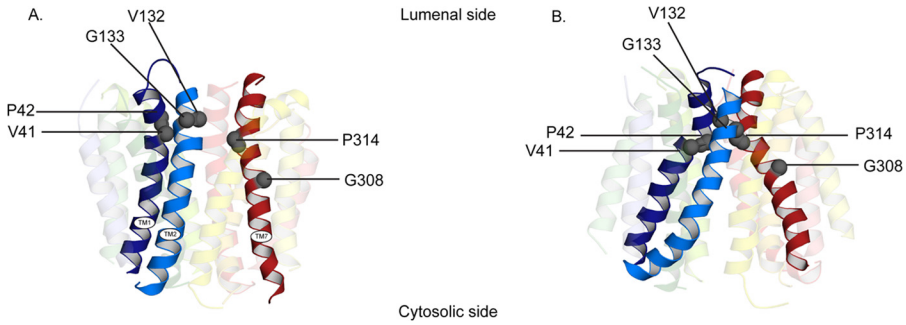

FIGURE 9. **Clustering of the mutations in the lumenal (*A*) and cytoplasmic (*B*) facing model of rVMAT2.** Helices are shown as schematics and viewed along the plane of the membrane with the cytoplasm to the bottom. The key helices, TM1, -2, and -7, are *opaque* and all the others are *transparent*.

formations of inverted-topology repeats (31, 32). Based on this paradigm, a vesicle-lumen facing conformation of rVMAT2 was generated by swapping the conformations of the repeat units in each half of the cytoplasm-facing structure (Fig. 9*A*) (15).

The mutations described in this work are clustered in TM1, -2, and -7 around the lumenal side of the molecule (Fig. 9, *A* and *B*). A visual comparison of the location of the mutated residues in the cytoplasm facing and the lumenal facing models hints to the possibility that they are part or somehow influence the lumenal gate. We report here that in many of the replacements identified, most notably in P314L, P314G, and V41A, a dramatic increase in K_m and V_{max} is observed. We suggest that this may be related to the effect of the mutations on the equilibrium between the conformations that may now favor the lumenal facing one and result in a faster transporter.

DISCUSSION

Early biochemical studies have shown that TBZ is a non-competitive inhibitor of transport and substrates inhibit TBZ binding only at concentrations 100 times higher than the K_m values for transport (11, 33). These findings have led Henry and co-workers (11) to suggest that TBZ binds at a site distinct from that of reserpine and the substrates, and that VMAT2 exists in two different conformations: TBZ-bound or substrate-bound (1). So far, the mechanism involved in the conformational changes necessary for TBZ binding remained unknown.

Determinants of TBZ Binding—To identify determinants of TBZ-binding affinity and specificity, we refined the method of directed evolution we previously established in *S. cerevisiae* (10). Thus, the mutagenic libraries we used in the present work were targeted to specifically defined regions of the *rVMAT2* gene. In addition, we used two structurally different substrates

of rVMAT2 for the screening experiments. The advantage of the approach described here is that it is unbiased by models or previous knowledge. It is therefore striking that our screen identified a cluster of "conformational" residues close to the lumenal side of the protein (Fig. 9). The mutants identified resulted from replacements in helix breakers, residues important in protein dynamics: a conserved Gly (Gly^{308}) and a conserved Pro (Pro^{314}), or in small Val residues, Val^{41} and Val^{132}, adjacent to conserved Pro and Gly positions, Pro^{42} and Gly^{133}. Our subsequent mutagenesis study on Pro^{42} and Gly^{133} demonstrated that they also play a role in TBZ binding and substrate transport. We speculate that the outcome of the mutations identified in positions Val^{41} and Val^{132} is due to their influence on the necessary flexibility conferred by the respective contiguous residues Pro^{42} and Gly^{133}. Indeed, the analysis of replacements of the highly conserved residues Pro^{42} and Gly^{133} support the essential role of these residues in the transport reaction. We previously demonstrated that the Pro residue equivalent to Pro^{42} is important also for the transport activity of the rVMAT1 isoform (26).

TM7—In the case of Gly^{308}, replacement of glycine to alanine with only an additional methyl almost completely eliminated the ability to bind TBZ by the transporter, whereas proline at this position fully restored TBZ sensitivity. The finding suggests that the requirement for an amino acid that allows flexibility of the helix at this position is essential for TBZ binding.

In the case of position 314, none of the mutants (Leu, Thr, and Gly replacements) were able to bind TBZ. Interestingly, Pro^{314} is positioned within the P*XX*P motif in TM7, which is fully conserved in the vesicular amine transporters and highly conserved in bacterial homologues in the MFS family (Fig. 4*C* and see also Ref. 32). Conservation of Pro^{314} and the P*XX*P motif suggests that this domain might be structurally and/or functionally important within vesicular amine transporters and related bacterial homologues. Pro^{314} is located two turns from Gly^{308} and is adjacent to Glu^{313}, a residue essential for serotonin transport and TBZ binding (15). In addition an A315T mutation reduced TBZ sensitivity of the transporter (20). These results provide support for the crucial involvement of TM7 in TBZ binding and serotonin transport.

TM1—The P*XX*P motif has been identified originally in TM1 (D2 motif in Refs. 24 and 25) a TM that is symmetric to TM7 in MFS transporters and in the model of rVMAT2 (15). Interestingly, Val^{41} is strategically situated and is adjacent to the first proline of the P*XX*P motif in TM1. The V41F mutant conferred weak but significant enough resistance to MPP^+ due to residual MPP^+ transport and seemed to have retained the ability to bind the competitive inhibitor reserpine as judged by the effect of the inhibitor on growth. However, the V41F mutant was completely devoid of serotonin transport activity and did not bind TBZ. We also observed a complete elimination of the capacity to support growth in the presence of acriflavine for this mutant, meaning that the identification of this residue was only possible on the MPP^+ background. These results validate our strategy of screening against two structurally different substrates. Furthermore, this finding highlights the power of the screen because even a marginal transport capacity confers to the yeast cell the ability to grow on the toxic substrate. This may be explained by the fact that the yeast vacuole is very large and even a slow removal from the cytoplasm, just somewhat faster than the leak from the medium, should be capable of reducing the concentration of the offending compound close to its target.

Interestingly, even relatively conservative replacements at position 41 failed to restore the ability of rVMAT2 to confer resistance against acriflavine even though they restored serotonin transport. Moreover, the results suggest that the nature of the side chain at this position is an important determinant in substrate and inhibitor recognition. Thus, the replacement with an aromatic amino acid (V41F) completely abrogated the ability to bind TBZ and produced transporters with impaired transport activity.

TM2—The mutations described here in TM2, Val^{132} and Gly^{133}, are strategically located close to Phe^{136}. We previously showed that replacement of Phe^{136} with Leu, Ile, Met, or Val resulted in decreased binding of TBZ (10). Further in TM2 we find Lys^{139} and Gln^{143}, two residues involved in interactions that provide important anchor points between the C- and N-domains, functioning as hinge points about which the two bundles flex and straighten to open and close the two pathways (15).

Based on our mutagenesis studies, biochemical analysis, and homology model of rVMAT2, a general mechanism of VMAT2 inhibition by TBZ can be proposed. We suggest that the inhibition of VMAT2 involves two major steps: initiation of the TBZ-bound conformation and immobilization of the transporter by generation of a dead-end complex of TBZ with the transporter.

Insight into the Mechanism of Transport—A good way to compare the catalytic efficiencies of different mutants by the same enzyme is to compare the ratio k_{cat}/K_m for the reactions. This parameter, sometimes called the specificity constant, is the rate constant for the conversion of the substrate to the product, in our case the transport from the cytoplasmic to the lumenal side of the membrane. Several of the replacements hereby identified produced increases in the K_m and V_{max} values. The most notable and highly significant increases were observed in the case of P314L, P314G, and V41A. The magnitude of these changes is well above the inherent variability from one proteoliposome batch to another. Simple time courses at one substrate concentration cannot detect changes of both kinetic parameters to a similar degree as in the cases reported here.

We suggest that this finding provides us with an interesting insight into the transport cycle. In all the active mutants characterized here, the ratio for V_{max}/K_m (proportional to the specificity constant) is quite similar to that of the wild type suggesting that the efficiency of the transport reaction is maintained in all of them. The increase in the K_m and V_{max} values may be related to the effect of the mutations on the rate-limiting step of the transport cycle. Because of the conformational nature of the residues and their clustering in the lumenal side of the membrane we speculate that the various replacements may have an effect on the equilibrium between the conformations that may now favor the lumenal facing one and result in a faster transporter. This may be due to changes in the flexibility of the protein in a way that bypasses or overcomes the rate-limiting step.

Studies in other MFS transporters, for example, LacY and FucP, indicate that residues such as the Pro equivalent to Pro^{42} (34) in TM1 and to Ala^{315} and Ile^{318} in TM7, play a primary role in gating the periplasmic cavity (35, 36). As above mentioned, a visual comparison of the location of the mutated residues in the cytoplasm facing and lumenal facing models hints to the possibility that they are part or somehow influence the lumenal gate. Furthermore, comparison of the homology models of rVMAT2 in the outward and inward facing conformations also implies that the P*XX*P motifs of TM1 and TM7 may participate in the gating-like movements of the transporter.

Another case of a 3-fold increase on the V_{max} was reported in the closely homologous rat vesicular acetylcholine transporter and was the result of a Gly replacement of Ala^{228} in TM5 (37). The authors suggested that the effect may be due to an increase in the flexibility of the Gly^{228}-Pro^{229} sequence generated by the mutation as compared with the Ala-Pro in the wild type. Residues in TM5 in rVMAT2 have also been shown to play a role in the interactions that allow the C- and N- terminal bundles flex and straighten to open and close the two pathways (15).

These studies provide the first glimpse into the mechanism of TBZ binding and inhibition. The findings support the role of conserved Gly and Pro residues in conformational changes that rVMAT2 undergoes for efficient binding of TBZ. At present a detailed assessment of the nature of the conformational changes is difficult to achieve because of the low expression level of rVMAT2 in *S. cerevisiae* and HEK293 cells. A more detailed understanding of the molecular basis for VMAT2-TBZ interaction and any associated conformational changes in the transporter will obviously require high-resolution structural studies of VMAT2 in different conformations and/or identification of prokaryotic homologues that express to higher levels and allow for documentation of structural changes with biochemical tools.

REFERENCES

1. Schuldiner, S., Shirvan, A., and Linial, M. (1995) Vesicular neurotransmitter transporters. From bacteria to humans. *Physiol. Rev.* **75,** 369–392
2. Eiden, L. E. (2000) The vesicular neurotransmitter transporters. Current perspectives and future prospects. *FASEB J.* **14,** 2396–2400
3. Blakely, R. D., and Edwards, R. H. (2012) Vesicular and plasma membrane transporters for neurotransmitters. *Cold Spring Harbor Perspect. Biol.* **4,** 10.1102/cshperspect.a005595
4. Parsons, S. M. (2000) Transport mechanisms in acetylcholine and monoamine storage. *FASEB J.* **14,** 2423–2434
5. Erickson, J. D., and Varoqui, H. (2000) Molecular analysis of vesicular amine transporter function and targeting to secretory organelles. *FASEB J.* **14,** 2450–2458
6. Chaudhry, F. A., Edwards, R. H., and Fonnum, F. (2008) Vesicular neurotransmitter transporters as targets for endogenous and exogenous toxic substances. *Annu. Rev. Pharmacol. Toxicol.* **48,** 277–301
7. Liu, Y., Peter, D., Roghani, A., Schuldiner, S., Privé, G. G., Eisenberg, D., Brecha, N., and Edwards, R. H. (1992) A cDNA that suppresses MPP^+ toxicity encodes a vesicular amine transporter. *Cell* **70,** 539–551
8. Yelin, R., and Schuldiner, S. (1995) The pharmacological profile of the vesicular monoamine transporter resembles that of multidrug transporters. *FEBS Lett.* **377,** 201–207
9. Schuldiner, S., Steiner-Mordoch, S., Yelin, R., Wall, S. C., and Rudnick, G. (1993) Amphetamine derivatives interact with both plasma membrane and secretory vesicle biogenic amine transporters. *Mol. Pharmacol.* **44,** 1227–1231
10. Gros, Y., and Schuldiner, S. (2010) Directed evolution reveals hidden properties of VMAT, a neurotransmitter transporter. *J. Biol. Chem.* **285,** 5076–5084
11. Scherman, D., Jaudon, P., and Henry, J. (1983) Characterization of the monoamine transporter of chromaffin granules by binding of [^{3}H]dihydrotetrabenazine. *Proc. Natl. Acad. Sci. U.S.A.* **80,** 584–588
12. Kenney, C., and Jankovic, J. (2006) Tetrabenazine in the treatment of hyperkinetic movement disorders. *Expert Rev. Neurother.* **6,** 7–17
13. Friedmann, Y., Shriki, A., Bennett, E. R., Golos, S., Diskin, R., Marbach, I., Bengal, E., and Engelberg, D. (2006) JX401, A p38α inhibitor containing a 4-benzylpiperidine motif, identified via a novel screening system in yeast. *Mol. Pharmacol.* **70,** 1395–1405
14. Elble, R. (1992) A simple and efficient procedure for transformation of yeasts. *BioTechniques* **13,** 18–20
15. Yaffe, D., Radestock, S., Shuster, Y., Forrest, L. R., and Schuldiner, S. (2013) Identification of molecular hinge points mediating alternating access in the vesicular monoamine transporter VMAT2. *Proc. Natl. Acad. Sci. U.S.A.* **110,** E1332–1341
16. Rogers, B., Decottignies, A., Kolaczkowski, M., Carvajal, E., Balzi, E., and Goffeau, A. (2001) The pleitropic drug ABC transporters from *Saccharomyces cerevisiae*. *J. Mol. Microbiol. Biotechnol.* **3,** 207–214
17. Adam, Y., Edwards, R. H., and Schuldiner, S. (2008) Expression and function of the rat vesicular monoamine transporter 2. *Am. J. Physiol. Cell Physiol.* **294,** 1004–1011
18. Sansom, M. S., and Weinstein, H. (2000) Hinges, swivels and switches. The role of prolines in signalling via transmembrane α-helices. *Trends Pharmacol. Sci.* **21,** 445–451
19. Finn, J. P., 3rd, and Edwards, R. H. (1997) Individual residues contribute to multiple differences in ligand recognition between vesicular monoamine transporters 1 and 2. *J. Biol. Chem.* **272,** 16301–16307
20. Finn, J. P., 3rd, and Edwards, R. H. (1998) Multiple residues contribute independently to differences in ligand recognition between vesicular monoamine transporters 1 and 2. *J. Biol. Chem.* **273,** 3943–3947
21. Darchen, F., Scherman, D., Desnos, C., and Henry, J.-P. (1988) Characteristics of the transport of the quaternary ammonium 1-methyl-4-phenylpyridinium by chromaffin granules. *Biochem. Pharmacol.* **37,** 4381–4387
22. Sievert, M. K., and Ruoho, A. E. (1997) Peptide mapping of the [^{125}I]iodoazidoketanserin and [^{125}I]2-*N*-[(3′-iodo-4′-azidophenyl)propionyl]tetrabenazine binding sites for the synaptic vesicle monoamine transporter. *J. Biol. Chem.* **272,** 26049–26055
23. Sagné, C., Isambert, M. F., Vandekerckhove, J., Henry, J. P., and Gasnier, B. (1997) The photoactivatable inhibitor 7-azido-8-iodoketanserin labels the N terminus of the vesicular monoamine transporter from bovine chromaffin granules. *Biochemistry* **36,** 3345–3352
24. Paulsen, I. T., Brown, M. H., and Skurray, R. A. (1996) Proton-dependent multidrug efflux systems. *Microbiol. Rev.* **60,** 575–608
25. Vardy, E., Steiner-Mordoch, S., and Schuldiner, S. (2005) Characterization of bacterial drug antiporters homologous to mammalian neurotransmitter transporters. *J. Bacteriol.* **187,** 7518–7525
26. Yelin, R., Steiner-Mordoch, S., Aroeti, B., and Schuldiner, S. (1998) Glycosylation of a vesicular monoamine transporter. A mutation in a conserved proline residue affects the activity, glycosylation, and localization of the transporter. *J. Neurochem.* **71,** 2518–2527
27. Huang, Y., Lemieux, M. J., Song, J., Auer, M., and Wang, D. N. (2003) Structure and mechanism of the glycerol-3-phosphate transporter from *Escherichia coli*. *Science* **301,** 616–620
28. Abramson, J., Smirnova, I., Kasho, V., Verner, G., Kaback, H. R., and Iwata, S. (2003) Structure and mechanism of the lactose permease of *Escherichia coli*. *Science* **301,** 610–615
29. Yan, N. (2013) Structural advances for the major facilitator superfamily (MFS) transporters. *Trends Biochem. Sci.* **38,** 151–159
30. Jardetzky, O. (1966) Simple allosteric model for membrane pumps. *Nature* **211,** 969–970
31. Forrest, L. R., and Rudnick, G. (2009) The rocking bundle. A mechanism for ion-coupled solute flux by symmetrical transporters. *Physiology* **24,** 377–386
32. Radestock, S., and Forrest, L. R. (2011) The alternating-access mechanism of MFS transporters arises from inverted-topology repeats. *J. Mol. Biol.*

407, 698–715
33. Scherman, D., and Henry, J. (1984) Reserpine binding to bovine chromaffin granule membranes. Characterization and comparison with dihydrotetrabenazine binding. *Mol. Pharmacol.* **25,** 113–122
34. Consler, T. G., Tsolas, O., and Kaback, H. R. (1991) Role of proline residues in the structure and function of a membrane transport protein. *Biochemistry* **30,** 1291–1298
35. Zhou, Y., Nie, Y., and Kaback, H. R. (2009) Residues gating the periplasmic pathway of LacY. *J. Mol. Biol.* **394,** 219–225
36. Sugihara, J., Sun, L., Yan, N., and Kaback, H. R. (2012) Dynamics of the L-fucose/H^+ symporter revealed by fluorescence spectroscopy. *Proc. Natl. Acad. Sci. U.S.A.* **109,** 14847–14851
37. Chandrasekaran, A., Ojeda, A. M., Kolmakova, N. G., and Parsons, S. M. (2006) Mutational and bioinformatics analysis of proline- and glycine-rich motifs in vesicular acetylcholine transporter. *J. Neurochem.* **98,** 1551–1559
38. Sievers, F., Wilm, A., Dineen, D., Gibson, T. J., Karplus, K., Li, W., Lopez, R., McWilliam, H., Remmert, M., Söding, J., Thompson, J. D., and Higgins, D. G. (2011) Fast, scalable generation of high-quality protein multiple sequence alignments using Clustal Omega. *Mol. Syst. Biol.* **7,** 539
39. Schneider, T. D., and Stephens, R. M. (1990) Sequence logos. A new way to display consensus sequences. *Nucleic Acids Res.* **18,** 6097–6100
40. Crooks, G. E., Hon, G., Chandonia, J. M., and Brenner, S. E. (2004) WebLogo. A sequence logo generator. *Genome Res.* **14,** 1188–1190